Defence Science Journal, Vol. 74, No. 2, March 2024, pp. 234-245, DOI : 10.14429/dsj.74.18256

Investigation of Multi-layered Mitigation Systems for Protection from 120 mm Mortar HE Top Attacks

Mohamed Abdelkhalik Aboelseoud* and Tamer Elshenawy

Technical Research Center, Cairo, Egypt
**E-mail: m.aboelseoud79@gmail.com*

ABSTRACT

This paper investigates the protection of reinforced concrete (RC) structures from Mortar 120 mm HE (high explosive) top attacks. Two multi-layered mitigation systems are proposed to be added to the roofs of RC structures to achieve full protection against the destructive effects of Mortar 120 mm (i.e., ballistic penetration and explosion). The proposed mitigation systems combine relatively high-strength materials to stop or slow down the projectile, along with lightweight porous materials to attenuate the explosion shock wave. The porous materials also serve to increase the thickness of the proposed mitigation systems, thereby increasing the explosion stand-off distance. Traditional construction materials such as steel and RC were used as cost-effective high-strength materials, while commercial rigid polyurethane foam and lightweight bricks were examined as shock wave absorbers. Two firing tests of the 120 mm bomb from cannon barrels were conducted against one-story RC structures strengthened with the proposed protection systems. A numerical simulation of the real firing tests was performed using the Autodyn hydrocode to further analyze the performance of the constituent components in mitigating the effects of the rounds. The current study demonstrates that the proposed mitigation systems, based on the concept of multi-layering, are efficient and have their merits in countering Mortar 120 mm HE attacks

Keywords: Mortar 120 mm HE; Ballistic penetration; Explosion; Dynamic firing test; Structure protection

1. INTRODUCTION

Numerous research studies have been conducted to evaluate the penetration and protective capabilities of urban concrete structures against various ballistic threats. These threats encompass shaped charges, shell ammunition, guided missiles, and mortar ammunition. Whelan[1] discussed the development of a new tandem conical-shaped charge system capable of defeating both double-reinforced concrete (RC) structures and heavy armor targets. The effectiveness of this shaped charge jet was demonstrated through the use of a flash X-ray system and firing trials conducted at different stand-off distances. Boulanger[2], *et al.* discussed the development of a 155 mm high explosive shell that could detonate after penetrating a hard concrete target with a thickness of up to 80cm. This study involved numerical modeling calculations and the selection of appropriate materials for the shell to achieve the desired objective. The validity of the proposed design was confirmed through static firing tests of a 155 mm HE shell projectile at zero incidence angle against a concrete target, with modifications made to the fuze to ensure detonation after concrete penetration. Patel[3] developed a functionally pre-engineered building shelter, both theoretically and experimentally, for rapid deployment in warzones to protect military personnel against indirect fire (IDF) attacks from mortars of various calibers (60, 80, 107, 120, and 160 mm. The theoretical analysis included LSDYNA blast loading analysis at different stand-off distances from the detonation point. A honeycomb protective layer was implemented to mitigate the blast wave generated by mortar high explosive detonation, while also protecting against fragments. However, the theoretical analysis did not investigate the resistance of the protective structure against mortar penetration, which could potentially cause more casualties than the blast damage itself.

Ngo[4], *et al.* studied the indirect effect of the blast loads generated from a terror car bomb on the structural analysis and its relevant structure dynamic response analysis. They have applied the characteristic pressure-impulse rule to tall buildings and concluded that a certain level of ductility can protect from the extreme blast loading applied to these tall buildings.

The Mortar 120 mm HE (high explosive) bomblet has been recently used in many terror attacks in the Middle East as IDF attacks. The bomb has been recently fired from cannon barrels against one-story military concrete structures causing severe damage and many casualties. Besides, the charge explosion took place after achieving ballistic penetration by the bomb, hence maximizing the round-destroying effects. The explosive charge of the used bomblets consisted of 2.25kg Trinitrotoluene(TNT) that is initiated via delayed-action fuze. Similar bombs were used during the firing tests of the current study. The bombs had a total mass of 12.6 kg, contained 2.25 kg of TNT, and combined delayed fuze action.

Received : 15 June 2022, Revised : 03 December 2023
Accepted : 23 January 2024, Online published : 26 March 2024

The bomblet's general specifications are also listed in detail in other references[5].

Wang[6], *et al.* performed Experiments and numerical simulation to study the destroying effects of different shaped charges on multi-layered targets consisting of concrete and pebble. The investigated shaped charges were initiated at different standoffs and had different configurations, liner wall thicknesses, and charge diameters. The results of this research clarified that the jetting projectile charge (JPC) and explosively formed projectile (EFP) have significantly different penetration effects on layered targets. EFP, with a charge of the same diameter as JPC, penetrated the examined targets with obviously larger hole diameters than JPC did. Nevertheless, JCP formed deeper holes in the layered targets than EFP at the same standoff distance.

Many studies have suggested retrofitting existing structural members via externally bonded Fiber-Reinforced Polymer (FRP) sheets for blast protection. Reviews for these studies are available in[7-8]. Although great advancement has been achieved in the fabrication of FRP composites, the cost of the FRP composites still prevents them from being cost-competitive with traditional concrete and steel elements. Moreover, externally bonded strengthening systems are prone to debonding failure, which precludes achieving the required strength[9].

Other studies have suggested protecting the existing structures against blast loads using sacrificial claddings[10-15]. A sacrificial cladding consists of a top skin, which works as a load distributor, an energy-absorbing core, and a rigid rear skin[16]. Some researchers examined sacrificial claddings that consist of a crushable core placed between the structure to be protected and a front skin only[15,17]. Crushable cores such as aluminum foam, polymeric foam, and honeycomb structures have been intensively studied[10,13,17-18]. Among these cores, polymeric foam ones are the most suitable choice for protecting RC buildings from the economic and ease of construction point of view.

Elshenawy[19], *et al.* discussed both the fragmentation[20] and blast load protection of current shelters from 120 mm mortar using laminated layers, but the bomblet-construction penetration interaction issue was not presented in that research.

The current research is dedicated to proposing sacrificial layers that can be added on the top of RC structures to save lives and mitigate the destructive effect of the Mortar 120 mm HE in such terror accidents. The weight of the proposed protection systems is an important factor that needs to be minimized to enable the application of these systems not only to future structures but also to the existing ones. The proposed multi-layered mitigation systems combined traditional construction materials such as steel and RC with crushable

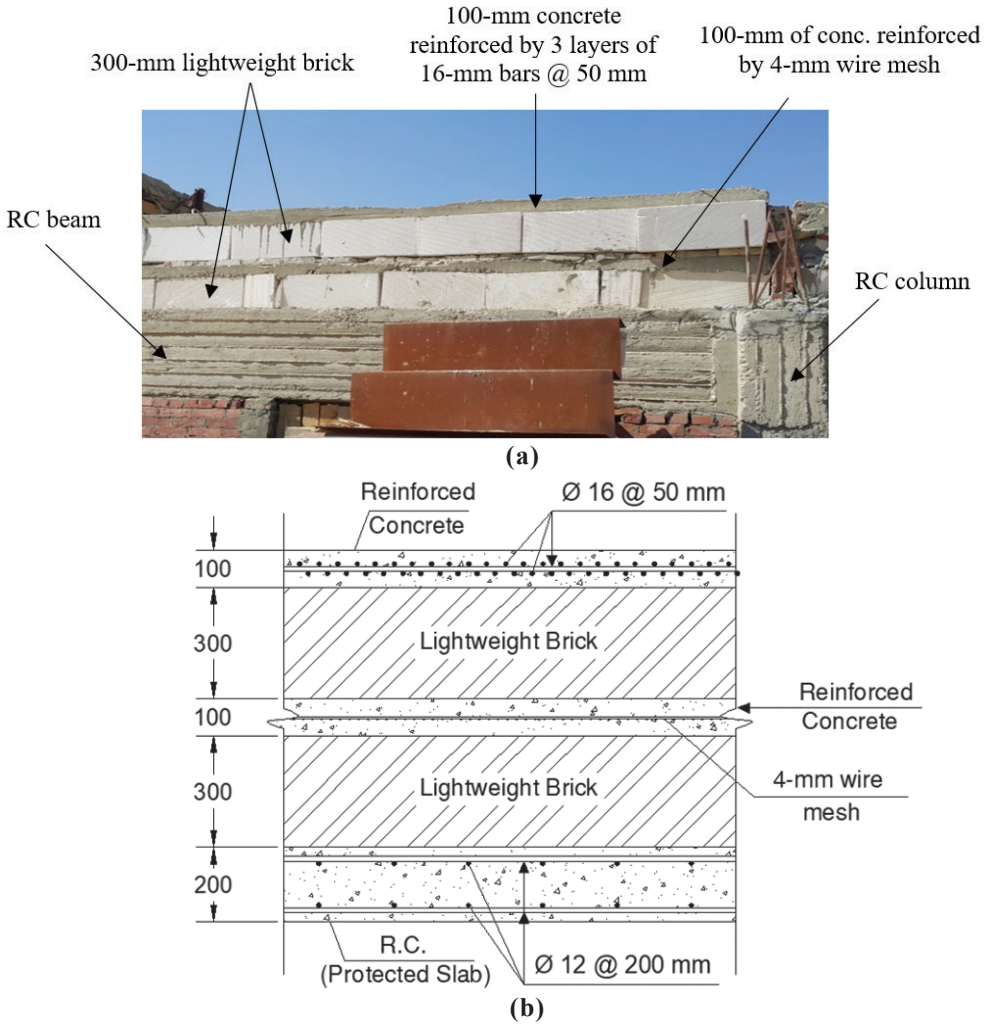

Figure 1. (a) First Mitigation system (MS1); and (b) Schematic drawing of the first mitigation system (MS1).

cores. Commercial rigid polyurethane foam was examined in the current study as a crushable core to absorb the Mortar 120 mm HE blast wave. The current research also investigated for the first time using commercial lightweight brick as a shock wave absorber. All the proposed systems aimed to achieve the following: 1) full protection against the Mortar 120 mm destroying effects (i.e. ballistic penetration and explosion effects, 2) ease of construction, 3) economic solution, and 4) a relatively light-weight system.

2. SIGNIFICANCE OF THE CURRENT RESEARCH

The primary goal of this work is to propose mitigation systems that can be added as sacrificial layers to RC structures in order to achieve full protection against mortar 120 mm HE attacks. The accuracy of unguided mortar 120 mm HE is 30 m [21], which makes dynamic firing tests of this type of bomb on structures complex, expensive, and time-consuming due to difficulties in target aiming. Therefore, numerical analysis of the effect of the 120 mm HE round on structures is crucial to minimize the need for experimental tests. The current research program includes the following activities:

- Proposing protection systems that can be integrated with both existing and future RC structures to protect them from the destructive effects of mortar 120 mm HE.
- Conducting two dynamic firing tests of mortar 120 mm HE on RC structures protected by two proposed mitigation systems. These tests involve examining two multi-layered mitigation systems as sacrificial layers added on top of two types of RC slabs: a thin slab with a total thickness of 140-mm and a thick slab that is 200-mm thick.
- Simulating the interaction between the bomblets and targets using Autodyn hydrocode to better evaluate the performance of the proposed mitigation systems in terms of mortar kinetic energy and target penetration.

3. EXPERIMENTAL TESTING PROGRAM

Two firing tests of the Mortar 120 mm HE from cannon barrels were conducted against two different structures, each of which was protected by a proposed mitigation system. The cannon was positioned 200 m away from the tested structures to minimize target-aiming misfire trials. Each structure had dimensions of 30x5 m^2. Thirteen firing trials were carried out to hit each structure only once.

The first mitigation system (MS1) consisted of four layers placed on a 200-mm RC slab supported by a traditional beam and column system (Fig. 1(a) & 1(b)). The first and third layers comprised 100-mm typical 250 kg/cm^2 concrete. The first layer was reinforced with three layers of 16-mm diameter typical 36/52 steel bars, spaced at 50-mm intervals in both directions. The third layer was reinforced with 4-mm diameter wire mesh. The second and fourth layers consisted of a 300-mm lightweight brick with a density of 90 kg/m^3. The total weight of MS1 was estimated to be 609 kg/m^2 (first layer's weight = 315 kg/m^2, third layer's weight = 240 kg/m^2, second and fourth layers' weight = 54 kg/m^2).

The second mitigation system (MS2) consisted of three layers placed on a 140-mm RC slab supported by a traditional beam and column system (Figs. 2-a & 2-b). Similar to MS1, the first layer was 100 mm of typical 250 kg/cm^2 concrete that was reinforced by three layers of 16-mm diameter reinforcing bars spaced at 50 mm. The second layer was comprised of four steel sub-layers: a 2-mm steel plate, 30x30x3 mm^3 steel angles spaced at 100 mm, a 2-mm steel plate, and 30x30x3 mm^3 steel angles spaced at 100 mm. The weight of the second layer was estimated to be 60 kg/m^2. The third layer was a 400-mm rigid polyurethane foam. The density of this foam is 160 kg/m^3. The total weight of MS2 was estimated to be 439 kg/m^2.

4. AUTODYN HYDROCODE MODELING

A hydrocode is a useful numerical tool that has been widely used to simulate dynamic problems that occur on a short time scale. In order to obtain the response of a continuous media subjected to dynamic loading via a hydrocode simulation, mass, momentum, and energy are assumed to remain constant within the problem domain, where the material is presented by its equation of state (EOS) and relevant strength model[22]. In the current research, Autodyn-3D hydrocode was utilized to simulate the interaction of the bomblet with the proposed mitigation systems. This simulation combines consecutive penetration and explosion interaction algorithms[23].

Although the mesh sensitivity has a significant effect on the numerical modeling results, it will not be included in the current research manuscript due to extensive meshing trials that have been applied to the laminated layers and the relevant numerical trials that have been conducted. These extensive meshing trials and relevant impacts on the penetration/protection may be published in separate research work.

The TNT charge of the bomblet under investigation initiates after 40 ms of impacting the target via delayed-action fuze. To minimize the computational effort, a preliminary penetration analysis of the round/target was carried out. This step aimed to identify the duration and the location at which the bomblet completely stops in each mitigation system before the detonation initiates. This duration was found to range from 2.0-3.0 ms approximately for all examined protection systems. A complete simulation that represents the consecutive penetration and explosion interactions was then performed for each examined mitigation system. In this simulation, the detonation started at a specific time and location that were determined from the exploratory penetration analysis. In the following sections, the penetration-blast simulation and the materials' models are briefly discussed.

4.1 Penetration-Blast Simulation

The bomblet was drawn via the 3D CAD package PTC Creo V3.0. The model was then meshed using the ANSYS R18.0 Workbench meshing tool and exported to ANSYS Autodyn R18.0. The bomblet was meshed to approximately 3200 elements. In the Autodyn model, all layers of MS1 and MS2 were constructed using Lagrange elements, except for the reinforcing bars, which were simulated using beam elements. Each element had a constant length of 10 mm.To optimize computational efficiency, only a representative section of the examined structure measuring 700 mm x 700 mm was included in the Autodyn model. The steel, brick, and foam parts were meshed with variable cell sizes in the y and z directions. The

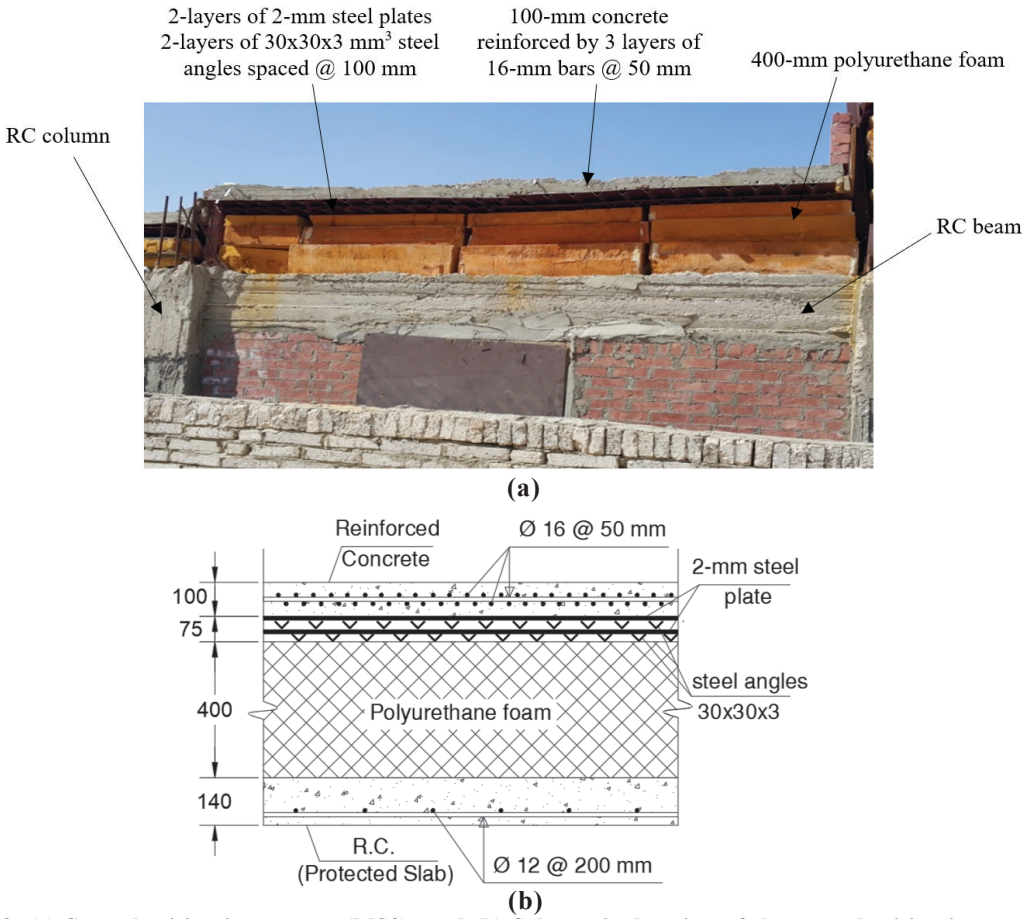

Figure 2. (a) Second mitigation system (MS2); and (b) Schematic drawing of the second mitigation system (MS2).

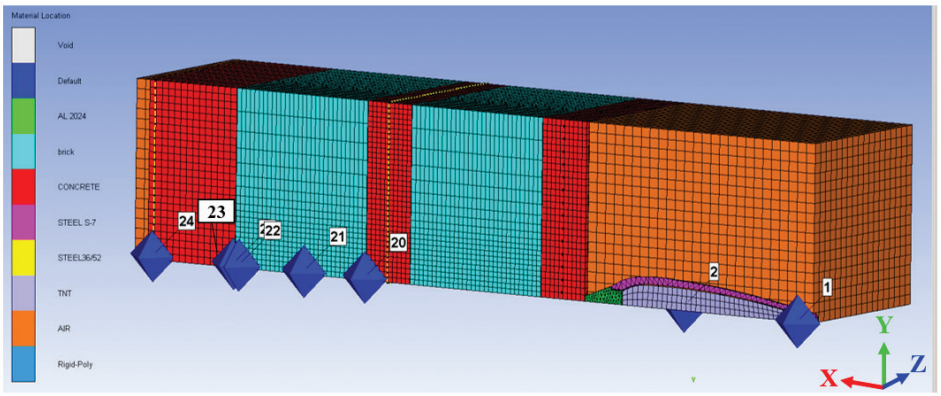

Figure 3. Modeling of Mortar 120 mm HE/MS1 interaction via AUTDYN-3D.

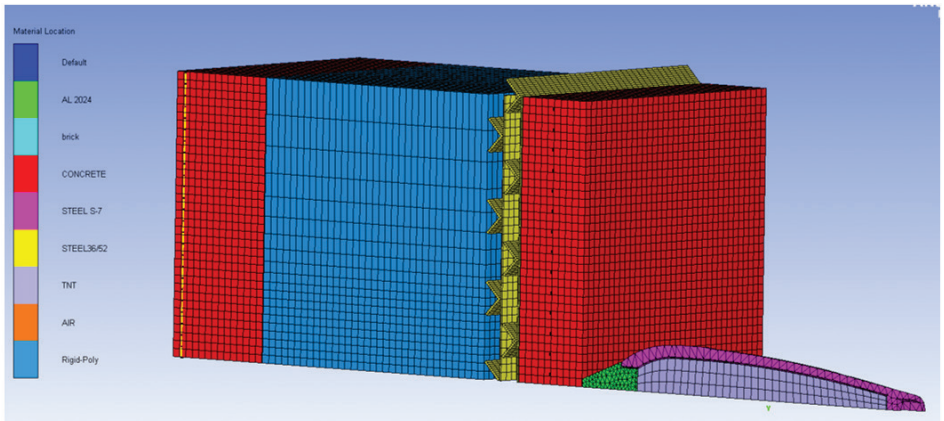

Figure 4. Modeling of Mortar 120 mm HE/MS2 interaction via AUTDYN-3D.

cell size gradually increased from 10 mm at the center to approximately 45 mm at the edges, resulting in a total of 40 cells in both directions.

The concrete parts were meshed with a constant cell size of 10 mm in the y and z directions to ensure that the reinforcing bars and concrete joints aligned. All Lagrangian parts, except for the air, were meshed with a constant size of 10 mm in the longitudinal (x) direction. Parts with a thickness of less than 10 mm were represented by a single cell in the longitudinal direction (x-dir.).The air part was meshed with a constant cell size of 20 mm in the x, y, and z directions.

Both the penetration and the blast loading of the bomblet were simulated using the Lagrange-Lagrange interaction scheme[23]. The impact velocity of the bomblet was set as an initial condition in the hydrocode simulation, estimated to be 140 m/s, which was confirmed by the radar used in the field testing facility. The bomblet's impact angle was assumed to be exactly 90° in the simulation. The Autodyn models for the bomblet's interaction with MS1 and MS2 are illustrated in Fig. 3 and Fig. 4, respectively.

4.2 Materials Modeling

The bomblet casing material was modeled as steel S-7, while the target's steel was modeled as steel 4340. Shock EOS was used for the bomblet's steel, the target's steel, and the aluminum during the numerical simulation. The strength model for both steel materials was Johnson-Cook (JC), while no strength model was specified for the aluminum. A detailed discussion of these models can be found in [22-24].The mechanical properties of the casing's steel and aluminum and the target's steel and foam are illustrated in Table 1.

Table 1. Mechanical properties of the bomblet's and target's materials [22].

Parameter	Steel S-7	Steel 4340	Al2024
Equation of state	Shock	Shock	Shock
Reference density (g/cm^3)	7.75	7.75	2.785
Gruneisen Coefficient	2.17	2.17	2.00
Parameter C_1 (m/s)	4569	4569	5328
Parameter s_1 (none)	1.49	1.49	1.338
Ref. temperature (K)	300	300	300
Strength model	JC	JC	
Constant A (kPa)	8.18×10^7	7.70×10^7	-
The hardening constant B (kPa)	4.77×10^5	7.92×10^5	
Hardening exponent; n (-)	0.18	0.26	
Strain rate constant (-)	0.012	0.014	
Thermal softening exponent (-)	1	1.03	-
Melting temperature T_m (K)	1763	1793	
Ref. strain rate (1/s)	1	1	

The concrete, foam, and brick materials were modeled by P-α EOS, which was presented by Herrmann[25]. The P-α model completely describes the porous material during the elastic, the plastic, and the fully compacted solid stages.

The strength model used for the concrete and brick was the RHT (Riedel-Hiermaier-Thoma) constitutive model[26]. This model combines plasticity and shear damage to describe the dynamic loading of brittle materials such as concrete. Further details of how the model represents the various aspects of the material behavior can be found in other references[26-28]. Boey[29] utilized the P-α compaction model along with the von Mises yield strength criterion to represent the rigid polyurethane foam dynamic behavior. The foam used in the current research (FR-6700 rigid polyurethane foam) is the same as the foam investigated in[29]. Subsequently, the input parameters for the foam were taken from[29]. The input parameters for the concrete, brick, and foam materials are listed in Table 2.

The equation of state (EOS) for employed TNT explosive charge is the "Jones Wilkins Lee" (JWL) equation. Experimental constants, for various explosives, have been determined from sideways plate push dynamic test experiments[30] and the cylinder expansion test[31-33]. Although plastic explosives[34]

Table 2. Input parameters for the RHT strength and failure model[36].

Material	Units	Concrete		Brick	Polyurethane foam
Strength	MPa	26	55	8	2.6
Equation of state		P-α			
Porous density	g/cm^3	2.30	2.35	0.09	0.16
Porous sound speed	m/s	2892	2981	2837	2490
Initial compaction pressure	MPa	17.3	36.6	5.3	2.6
Solid compaction pressure	GPa	6	6	6	0.11254
Compaction exponent	-	3	3	3	1.56
Strength		RHT Concrete			von Mises
Shear Modulus	GPa	16.2	17.7	15.3	$19.36*10^{-3}$
Yield stress	MPa	-	-	-	2.60
Compressive strength (f_c)	MPa	26	55	8	-
Tensile strength (f_t/f_c)	-	0.1	0.1	0.1	-
Shear strength (f_s/f_c)	-	0.18	0.18	0.18	-
Compressive strain rate exp. δ	-	0.034	0.028	0.038	-
Tensile strain rate exp. α	-	0.038	0.032	0.042	-

and plastic bonded explosives[35] showed better stability and performance than those of the TNT baseline explosive charge, the TNT military-grade explosive charge is still used to fill the 120 mm mortar charge. TNT explosive loading density was 1.63 g/cm^3. Parameters A, B, ω, R_1, and R_2 in the JWL EOS equation equal 3.7377×10^8kPa, 3.7471×10^6kPa, 0.35, 4.15, and 0.9; respectively. The Detonation velocity equals 6930 m/s and the detonation pressure equals 2.1×10^7kPa. The C-J energy per unit volume is equal to 6.0×10^6 kJ/m^3. These data have been retrieved from the Autodyn library.

Figure 5. First RC layer of MS1 after performing the firing test.

Figure 6. Structure protected by MS1 from the inside after performing the firing test.

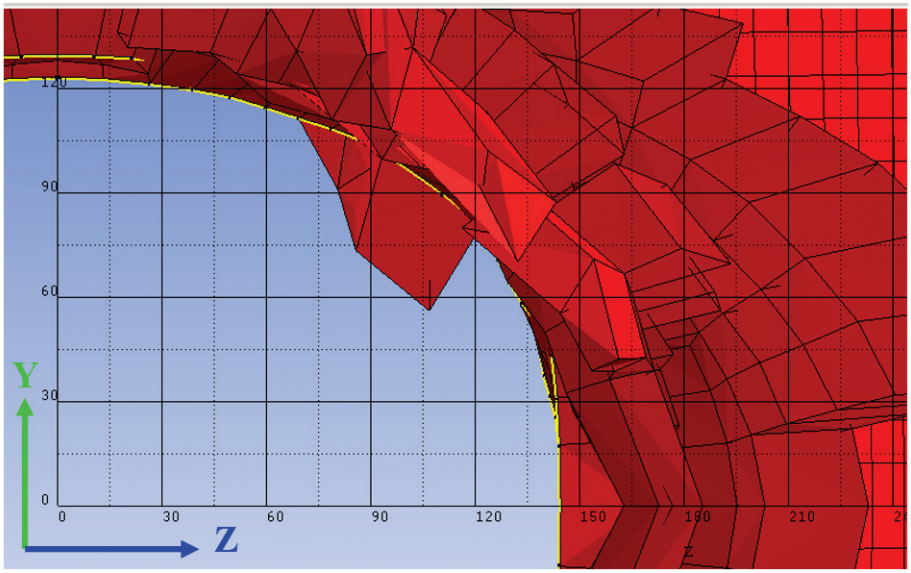

Figure 7. Radius of the aperture that took place in thefirst RC layer of MS1 due to the bomblet-destroying effect (Autodyn simulation).

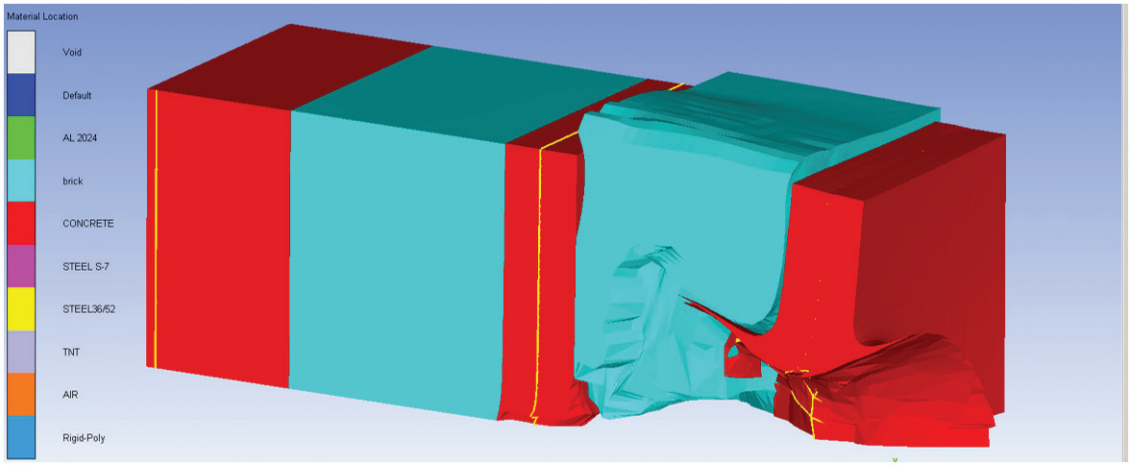

Figure 8. Damage that occurred in MS1 due to the bomblet-destroying effect.

equation equal 3.7377×10^{8} kPa, 3.7471×10^{6} kPa, 0.35, 4.15, and 0.9; respectively. The Detonation velocity equals 6930 m/s and the detonation pressure equals 2.1×10^{7} kPa. The C-J energy per unit volume is equal to 6.0×10^{6} kJ/m^3. These data have been retrieved from the Autodyn library.

5. RESULTS ANALYSIS AND DISCUSSION

The experimental and theoretical results of the bomblet/MS1 interaction are illustrated in Fig. 5 through 11. The firing test results clarified that the bomb penetration/explosion effects resulted in an aperture in the concrete of the first layer with an average diameter of approximately 300 mm (Fig. 5). The inspection of the tested MS1 showed that the bomb effect was confined to the third layer, with a total damage depth of approximately 440 mm from the top of MS1 (i.e., the bomb effect reached 40 mm in the third layer). To roughly determine the depth of the affected layers, a thin rod was passed through the hole in the tested structure until it got stuck. The length of the penetrated part of the bar was then measured, identifying approximately the depth of the damage resulting from the bomblet attack. As shown in Fig. 5, the bottom of the RC slab was completely unaffected by the 120 mm mortar attack. The building's window was also found to be intact, without any damage or cracks observed on the glass. These observations clarify that the proposed laminated layers were able to safely protect the attacked RC structure.

The results of the numerical simulation were in agreement with the findings from the experimental testing. According to the simulation, the bomblet caused an aperture in the first RC layer with an average diameter of 270 mm, as shown in Fig. 7. However, the real reinforcing bars were found to be less affected compared to the bars in the numerical simulation. The penetration/explosion of the round TNT charge was observed to cause a total damage depth of approximately 490 mm, reaching 90 mm into the third layer. The bottom of the RC slab was found to be unaffected, which aligns with the observations from the experimental testing, as shown in Fig. 8.

The location of the bomblet at t = 2.48 ms,during the bomblet/MS1 interaction, is displayed in Fig. 9. At this time, the velocity of the bomblet was predicted in the simulation to be zero (Fig. 10). This result clarifies that the reinforcing bars in the first RC layer were able to arrest the bomb and bring it to rest before the bomblet explosion. The geometry and the diameter of the aperture in the reinforcing bars shown in Fig. 5 suggest that the bomb was stopped at the face of the reinforcing bars, as detected by the Autodyn model. The same behavior was numerically detected during the bomblet/MS2 interaction. These results demonstrate that reinforcing the first concrete

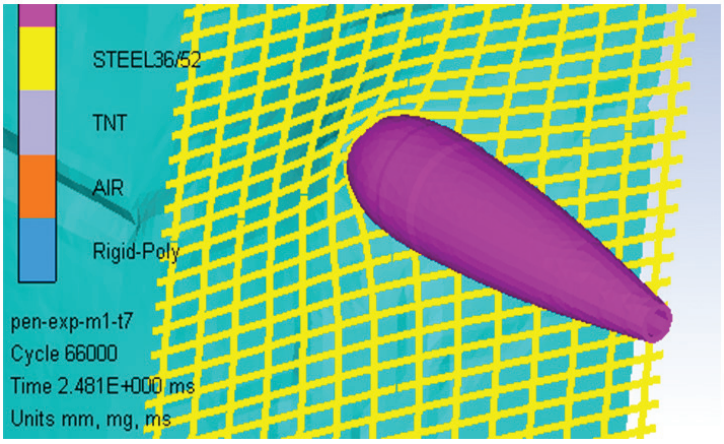

Figure 9. The Mortar 120 mm/M 1 interaction at t = 2.48 ms.

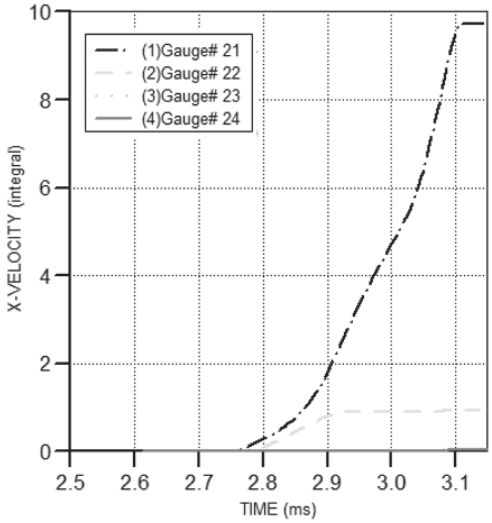

Figure 11. Estimated deflection (in mm) at different locations (gages 21, 22, 23, and 24) in MS1 due to the Mortar 120 mm effects.

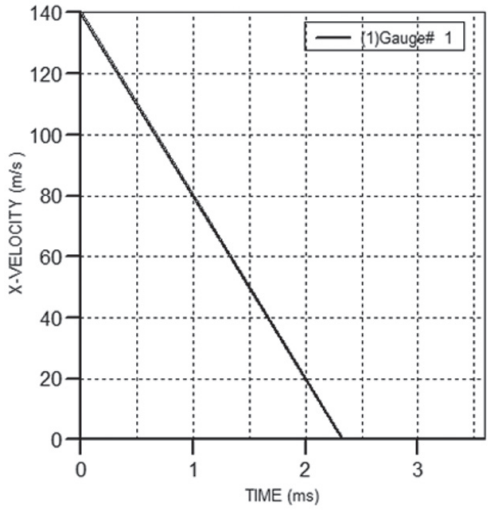

Figure 10. Velocity estimated by the simulation at the bomblet tail (gage 1).

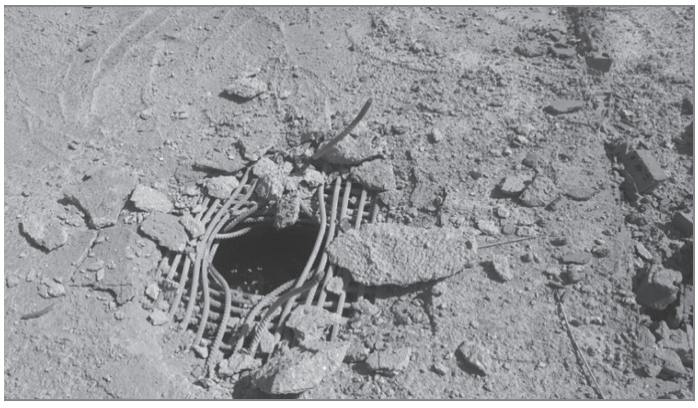

Figure 12. First RC layer of MS2 after performing the firing test.

layer with three layers of 16 mm bars is useful in defeating the penetration effect of the Mortar 120 mm. Arresting the bomb with the steel bars also alleviates the explosion effect by increasing the explosion standoff distance.

The deflections predicted at the mid and end of the fourth layer (brick layer) [gages 21 and 22, respectively], and at the start and end of the slab (gages 23 and 24, respectively), are shown in Fig. (11). Gage 21 is located approximately 650 mm from the top of MS1, gage 22 is located approximately 795 mm from the top of MS1 (5 mm before the end of the fourth layer), gage 23 is located approximately 810 mm from the top of MS1 (10 mm below the top of the protected slab), and gage 24 is located approximately 1000 mm from the top of MS1 (at the bottom of the protected slab).

As shown in Fig. 11, the slab exhibited almost no deflection due to the bomb-destroying effect (the curves of gages 23 and 24 are approximately identical, thus only the curve of gage 24 can be seen in Fig. 11). These results align with experimental observations, confirming that the proposed MS1 is efficient in protecting the examined RC structure from Mortar 120mm HE attacks. The predicted deflections also illustrate that the fourth layer and the slab did not experience any deflections before 2.5 ms (i.e., before the initiation of the explosion). The difference between the deformations at the mid and end of the brick (gages # 21 and 22) also indicates that the brick was compressed due to the bomblet detonation, suggesting its effectiveness in mitigating the detonation effect.

The field testing and simulation results of the bomblet/MS2 interaction are presented in Figures 12 through 15. The average diameter of perforations in the reinforcing bars of the first layer was approximately 270 mm in experimental testing and 200 mm in numerical analysis (Figures 12, 13-a & 13-b). Similarly, the damaged concrete area in this layer was significantly larger in the real case than in the numerical simulation.

Fire testing demonstrated that the bomblet affected all MS2 layers, resulting in slight damage to the RC slab Fig. 14. A similar result was predicted by the Autodyn model Fig. 15. However, in the numerical model, the damaged area in the concrete cover was significantly smaller. The geometry and diameter of the apertures in the concrete and steel bars in Fig. (12) (the reinforcing bars showed primarily lateral deformations) suggest that the bomb likely stopped between the reinforcing bars, not at the bars' top as detected by the

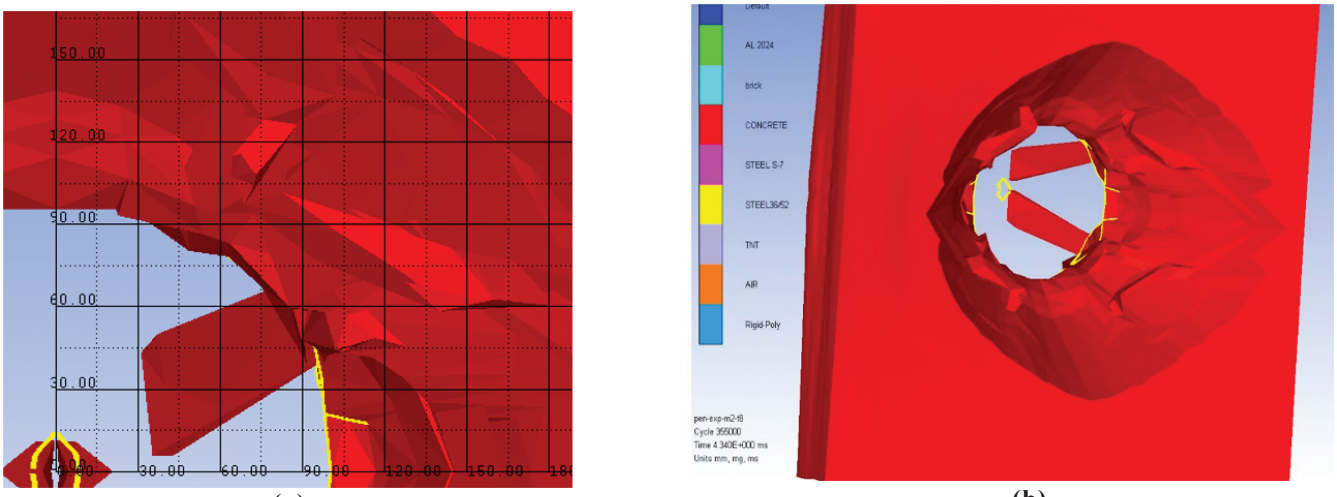

(a) **(b)**

Figure 13. (a) Aperture in the first RC layer of MS2 as predicted by the Autodyn simulation due to the bomblet effect (2D-view); and (b) The aperture in thefirst RC layer of MS2 as predicted by the Autodyn simulation due to the bomblet effect (3D-view).

Figure 14. Structure protected by MS2 from inside after performing the firing test.

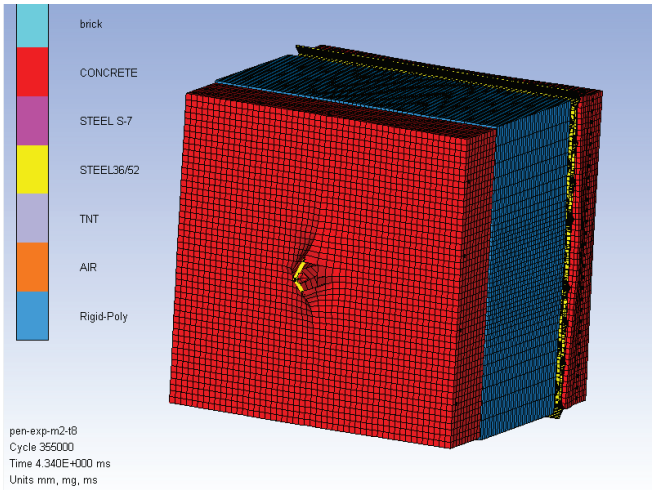

Figure 15. Penetration/explosion interaction between the mortar 120 mm bomblet and MS2 (Autodyn Simulation).

simulation. This explains the larger damaged areas in real testing compared to the simulation.

Two reasons might contribute to the difference between the numerical and experimental results of MS2. First, firing tests were conducted 28 and 12 days after pouring the concrete for the first layer of MS1 and MS2, respectively. Consequently, MS2's first layer likely had less concrete strength than MS1's first layer, despite an identical concrete mix, explaining why the bomblet didn't stop at the top of the first layer's reinforcing bars in MS2. Second, during the firing test at MS2, the foam (second layer) caught fire due to the bomblet explosion, potentially reducing the efficiency of the foam in attenuating the explosion wave.

In general, the disparities between theoretical observations and experimental results can be attributed to several factors, including variations in the actual and theoretical projectile impact angles, differences in material properties used in Autodyn analyses and the real materials' properties of constructed structures, and the accuracy of measuring the depth of damaged layers on-site. However, the numerical analysis results show an acceptable agreement with the results of real firing tests. Consequently, numerical simulation was employed to analyze the behavior of constituting elements during bomblet/target interactions (Tu and Lu, 2009; Riedel, 1999). It was also utilized to propose alternative protection systems for MS2, aiming to enhance protection against Mortar 120 mm HE attacks.

To compare the performance of the rigid polyurethane foam and the lightweight brick in absorbing the shock wave, a numerical simulation for the effect of the bomblet on a system similar to MS2 was executed. However, in this system, the third layer was 40 mm lightweight brick instead of foam resulting in a total system weight of 411 kg/m^2.

The total energy absorbed by the brick and the foam is displayed in figures (16-a &16-b). This simulation clarified that the foam absorbed energy about three times larger than the brick. However, the brick is significantly lighter than the foam. Thus, the brick can be a good solution when there are no constraints on the total depth of the protection layers because a brick layer of the same weight as a foam layer is almost two times thicker, which increases the bomblet explosion stand-off distance. The lightweight brick also provides another advantage over the foam because, unlike the foam, the brick is invulnerable to ignition under the explosion of the bomblet.

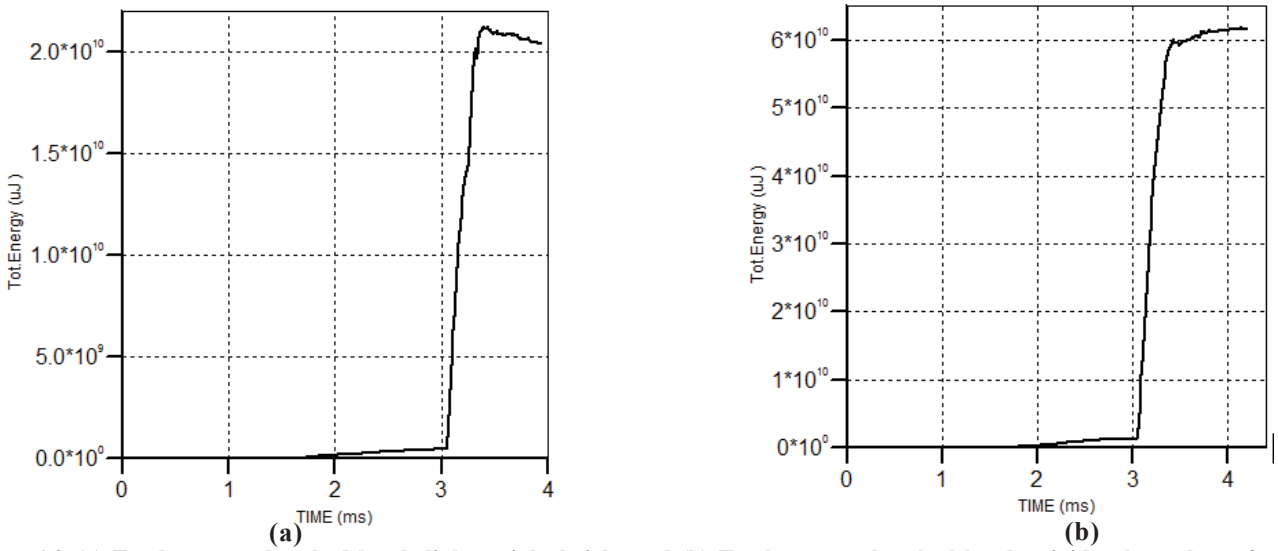

Figure 16. (a) Total energy absorbed by thelight weight brick; and (b) Total energy absorbed by the rigid polyurethane foam.

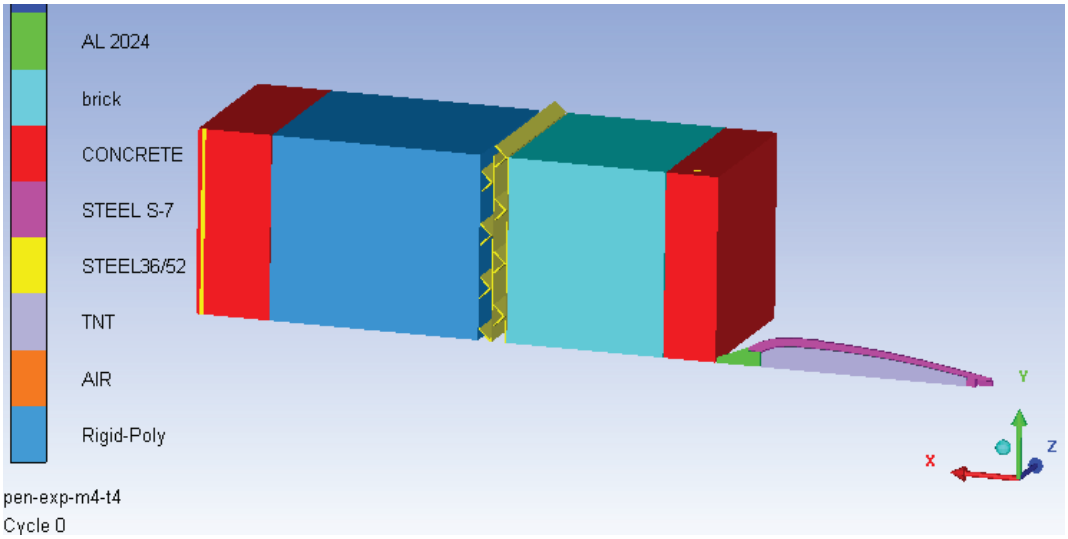

Figure 17. Modeling of Mortar 120mm HE/MS3 interaction via AUTDYN-3D.

Thus, placing the foam close to the top of the mitigation system is not recommended.

Two systems (MS3 and MS4) were studied as alternatives for MS2 to be added as sacrificial layers on RC structures. The design of these systems was based on the conclusions drawn from both the experimental tests and the numerical simulations of MS1 and MS2. As it was demonstrated, the lightweight brick and the polyurethane foam proved to be effective in mitigating the bomb's detonation wave. However, it was noted that foam is susceptible to ignition when the explosion occurs in close proximity. Moreover, the brick was the lightest material among the investigated ones (steel, concrete, foam, and brick). Consequently, MS3 (Fig. 17) was designed to be similar to MS2 but with an extra layer of 300-mm brick added directly below the 100-mm RC layer (first layer). The additional brick layer weighs approximately 27 kg/m^2 allowing MS3 (which weighs 466 kg/m^2) to be integrated with both new structures and existing ones. The addition of this layer is useful in absorbing the detonation wave energy and increasing the explosion stand-off distance not only for the protected slab but also for the polyurethane foam, hence maximizing the benefit of the foam layer. As a result, MS3 was found to be able to protect the 140 mm-slab from the bomblet attack.

The RC layer that is reinforced by three layers of 16-mm diameter was proved to be useful in defeating the bomblet's penetration of the proposed sacrificial layers. The proposed system MS4 aims to compare the performance of this layer and a steel layer, of the same weight, consisting of steel plates and angles. Thus, MS4 (Fig. 18) is similar to MS3 except for the first layer. In MS4, the first layer consists of ten 2-mm plate layers alternating with ten 30x30x3 mm^3 steel angle layers and weighs approximately 30 kg/m^2.

MS4 was proved to be able to safely protect the 140mm-slab from the bomblet effect. Nevertheless, it was found to have slightly better performance than MS3. This may be attributed to the configuration of the first layer of MS4. This configuration allowed part of the detonation wave to be laterally dissipated (i.e. this layer behaved to some extent similar to pours materials). Whereas, the configuration of the first RC layer in MS3 resulted in the confinement of the explosion wave. As a consequence, the wave was directed only in the longitudinal direction transmitting higher energy to the

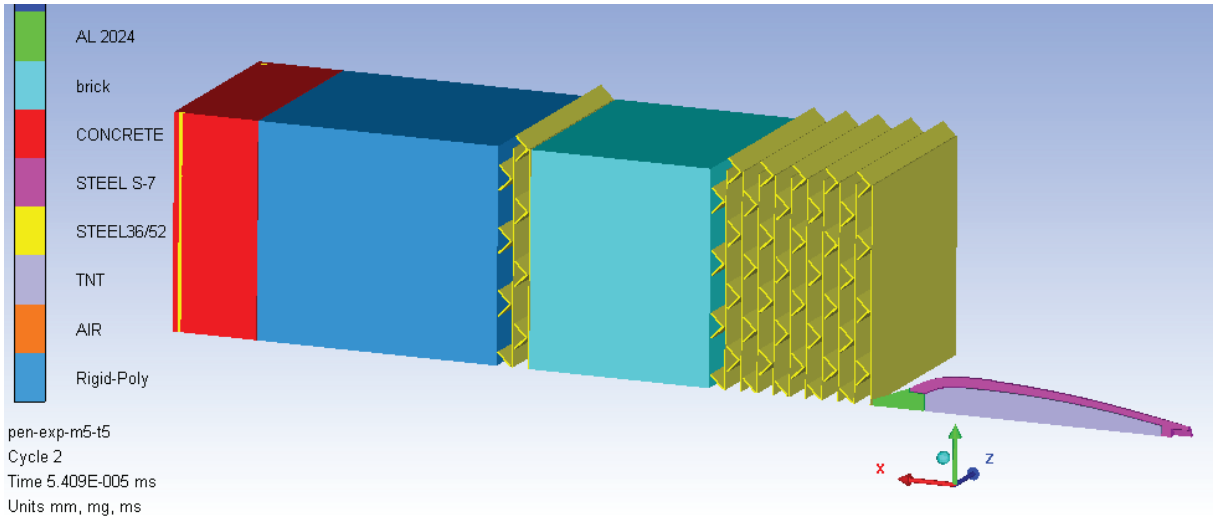

Figure 18. Modeling of mortar 120 mm HE/MS4 interaction via AUTDYN-3D.

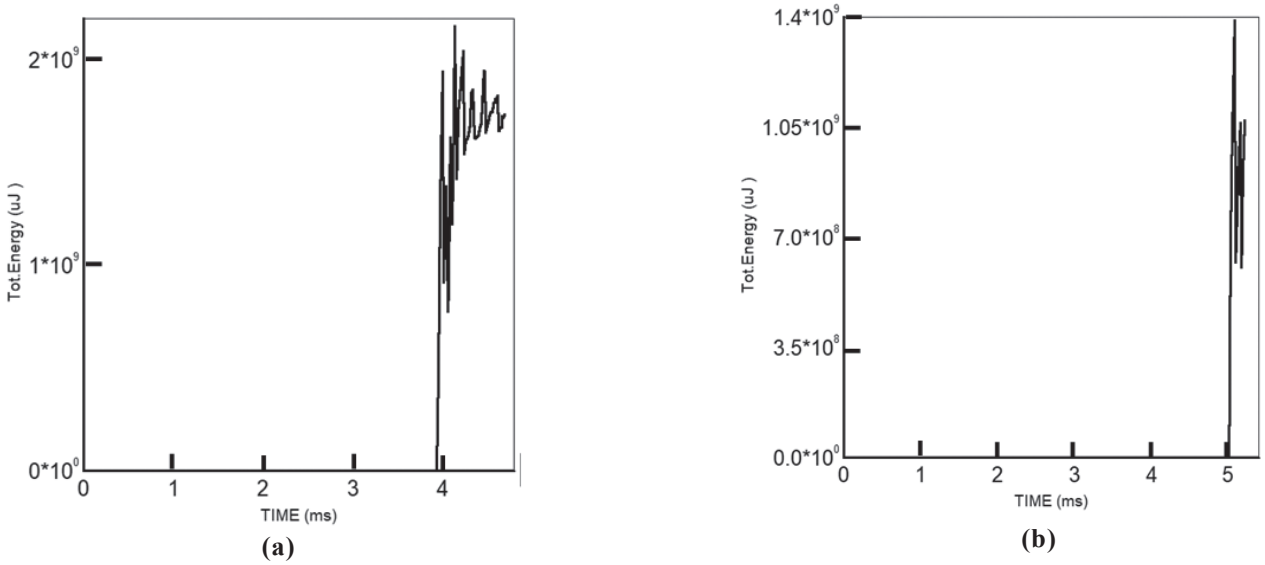

Figure 19. (a) Total energy absorbed by the protected RC slab of MS3 and (b) Total energy absorbed by the protected RC slab of MS4.

remaining protection layers and the RC slab than those of MS4. The results displayed in Fig. 19(a) & Fig. 19(b) assure this behavior. These two figures illustrate that the slab protected by MS4 was less affected by the bomblet attack than the slab protected by MS3. The deflections predicted at the bottom of RC slabs protected by MS3 and MS4 were 0.15 mm and 0.08 mm, respectively. These deflections are in agreement with the conclusions that both systems are capable of protecting the targeted structures, while MS4 behaves slightly better than MS3 in defeating the Mortar 120mm HE attacks.

6. CONCLUSIONS

This research program focuses on studying the protection of military RC structures against mortar 120mm HE terror attacks. To achieve full protection against these strikes, several mitigation systems have been proposed. These systems involve adding sacrificial layers on top of RC structures, combining high-strength materials such as steel and RC with lightweight porous materials like commercial rigid polyurethane foam and lightweight brick. The effectiveness of these proposed protection systems was evaluated through experimental examination and numerical simulation.

The experimental examination involved conducting two firing tests of unguided mortar 120mm HE against RC structures protected with the proposed mitigation systems. Additionally, numerical simulations using the 3D Autodyn hydrocode were performed to simulate the interaction between the bomblets and targets. Both the experimental and theoretical results demonstrated the efficiency of the proposed systems in protecting RC structures from mortar 120mm HE attacks.The results of this study showed that the high-strength materials were capable of stopping the projectile, while the porous materials effectively absorbed the detonation shock wave, thereby achieving complete protection against the destructive effects of the mortar 120mm HE.

REFERENCES

1. Whelan, A.J. Multiple effect warheads for defeat of urban structures and armour. In Proceedings of the 24th International Symposium on Ballistics, New Orleans, Louisiana, 2008, pp 1092-1098.
2. Boulanger, R.J.; A. V. & Hoff, D. An artillery shell for anti-bunker applications (155 ABS). In 22nd International Symposium, Ballistics. Vancouver, Canada, 2005, pp 593-601
3. Patel, K.M. Exploration of expeditious pre-engineered building system subject to mortar attacks. Master thesis, California State University, 2018.
4. Ngo, T.; *et al.* Blast Loading and Blast Effects on Structures–an Overview. *Electron. J. Struct. Eng.*, 2007, **7**(S1), 76-91.
5. Berko Zecevic, A.C.; Jasmin, Terzic & Sabina, Serdarevic Kadic. Analysis of influencing factors of mortar projectile reproduction process on fragment mass distribution. In 13th Seminar New Trends in Research of Energetic Materials. University of Pardubice, Pardubice, Czech Republic, 2010.
6. Wang, C.; Xu, W. & Li, T. Experimental and numerical studies on penetration of shaped charge into concrete and pebble layered targets. *Int. J. Multiphysics*, 2017, **11**(3), 295-314. doi: 10.21152/1750-9548.11.3.295
7. Pham, T.M. & Hao, H. Review of concrete structures strengthened with FRP against impact loading. *Structures*, 2016, **7**, 59-70. doi:10.1016/j.istruc.2016.05.003.
8. Buchan, P.A. & Chen, J.F. Blast resistance of FRP composites and polymer strengthened concrete and masonry structures–A state-of-the-art review. *Composites Part B: Eng.*, 2007, **38**(5-6), 509-522. doi: 10.1016/j.compositesb.2006.07.009.
9. Tang, T. & Saadatmanesh, H. Behavior of concrete beams strengthened with fiber-reinforced polymer laminates under impact loading. *J. Composites for Construct.*, 2003, **7**(3), 209-218. doi: 10.1061/(ASCE)1090-0268(2003)7:3(209).
10. Aminou, A.; Belkassem, B.; Atoui, O.; Lecompte, D. & Pyl, L. Numerical modeling of brittle mineral foam in a sacrificial cladding under blast loading. In Congrès Français de Mécanique CFM 2022: Congrès Français de Mécanique CFM, 2022.
11. Blanc, L.; Schunck, T. & Eckenfels, D. Sacrificial cladding with brittle materials for blast protection. *Materials*, 2021, **14**(14), 3980. doi: 10.3390/ma14143980.
12. Brekken, K.A.; Reyes, A.; Berstad, T.; Langseth, M. & Børvik, T. Sandwich panels with polymeric foam cores exposed to blast loading: An experimental and numerical investigation. *Appl. Sci.*, 2020, **10**(24), 9061. doi:10.3390/app10249061.
13. Sun, G.; Wang, E.; Zhang, J.; Li, S.; Zhang, Y. & Li, Q. Experimental study on the dynamic responses of foam sandwich panels with different facesheets and core gradients subjected to blast impulse. *Int. J. Impact Eng.*, 2020, **135**, 03327. doi: 10.1016/j.ijimpeng.2019.103327.
14. Jonet, A.; Belkassem, B.; Atoui, O.; Pyl, L. & Lecompt, D. Blast mitigation using brittle foam based sacrificial cladding: A feasibility study. *In* 18th International Symposium for the Interaction of the Effect of Munitions with Structures, 2019.
15. Ousji, H.; Belkassem, B.; Louar, M.A.; Reymen, B.; Pyl, L. & Vantomme, J. Experimental study of the effectiveness of sacrificial cladding using polymeric foams as crushable core with a simply supported steel beam. *Adv. Civil Eng.*, 2016. doi: 10.1155/2016/8301517.
16. Yuen, S.C.K.; Cunliffe, G. & Du Plessis, M.C. . Blast response of cladding sandwich panels with tubular cores. *Int. J. Impact Eng.*, 2017, **7**, 266-278. doi: 10.1016/j.ijimpeng.2017.04.016.
17. Langdon, G.S.; Karagiozova, D.; Theobald, M.D.; Nurick, G.N.; Lu, G. & Merrett, R.P. Fracture of aluminum foam core sacrificial cladding subjected to air-blast loading. *Int. J. Impact Eng.*, 2010, **37**(6), 638-651. doi: 10.1016/j.ijimpeng.2009.07.006

18. Liu, H.; Cao, Z.K.; Yao, G.C.; Luo, H.J. & Zu, G.Y.. Performance of aluminum foam–steel panel sandwich composites subjected to blast loading. *Materials and Design*, 2013, **47**, 483-488. doi: 10.1016/j.matdes.2012.12.003
19. Elshenawy, T.; M.A., Seoud. & G., Abdo. Ballistic protection of military shelters from mortar fragmentation and blast effects using a multi-layer structure. *Def. Sc. J.*, 2019, **69**(6), 538-544. doi: 10.14429/dsj.69.13269.
20. Sterne, T. A note on the Initial Velocities of Fragments from Warheads. BRL Report, 1947, 648.
21. Trohanowsky, R. 120 mm mortar system accuracy analysis. in address. International Infantry & Joint Services Small Arms System Annual Symposium, Exhibition & Firing Demonstration, 2005, Vol. 17.
22. A. Team. Autodyn Theory Mnaua. Revision, 3 ed. CA, Century Dynamics, 1997.
23. Dnamics, C. AUTODYN Compendium of Papers C. Dnamics, Editor. 1985, USA.
24. Johnson, G. & Cook, W. A constitutive model and data for metals subjected to large strains, high strain rates and high temperatures. In Proc. 7th Int. symposium on ballistics, 1983, pp 541-547.
25. Herrmann W. Constitutive equation for the dynamic compaction of ductile porous materials. *J. Appl. Physics*, 1968, **40**(6), 2490-2499. doi:10.1063/1.1658021
26. Grunwald, C.; Schaufelberger, B.; Stolz, A.; Riedel, W. & Borrvall, T. A general concrete model in hydrocodes: Verification and validation of the Riedel–Hiermaier–Thoma model in LS-DYNA. *Int. J. Protective Struct.*, 2017, **8**(1), 58-85. doi:10.1177/2041419617695977
27. Elshenawy, T. & Q., Li. Influences of target strength and confinement on the penetration depth of an oil well perforator. *Int. J. Impact Eng.*, 2013, **54**, 130-137. doi:10.1016/j.ijimpeng.2012.10.010
28. Berg, V. & Preece, D. Shaped charge induced concrete damage predictions using RHT constitutive modeling. In Proceedings of the Annual Conference on Explosives and Blasting Technique, 2004, 2, 261-272.
29. Boey, C.W. Investigation of shock wave attenuation in porous materials. Doctoral dissertation, Monterey, California. Naval Postgraduate School.2009, 16.
30. Tarver, C.M.; Tao, W.C. & Lee., C.G. Sideways plate push test for detonating solid Explosives. *Propellants, Explosives, Pyrotechnics*, 1996, **21**(5), 238-246. doi:10.1002/prep.19960210506.
31. Lan, I.; Hung, S.C.; Chen, C.Y.; Niu, Y.M. & Shiuan, J.H. An improved simple method of deducing JWL parameters from cylinder expansion test. *Propellants, Explosives, Pyrotechnics*, 1993, **18**(1), 18-24. doi:10.1002/prep.19930180104
32. Elek, P.M.; Džingalašević, V.V.; Jaramaz, S.S. & Micković, D.M. Determination of detonation products equation of state from cylinder test: Analytical model and numerical analysis. *Thermal Sci.*, 2015, **19**(1), 35-48. doi: 10.2298/TSCI121029138E
33. Kato, H.; Kaga, N.; Takizuka, M.; Hamashima, H. & Itoh, S. Research on the JWL parameters of several kinds of explosives. In Materials Science Forum, 2004, **465**, 271-276. Trans Tech Publications Ltd. doi:10.4028/www.scientific.net/MSF.465-466.271
34. Elbeih, A.; Elshenawy, T.; Amin, H.; Hussein, A.K. & Hammad, S.M. Preparation and characterization of a new high-performance plastic explosive in comparison with traditional types. *Int. J. Chem. Eng.*, 2019. doi: 10.1155/2019/4017068
35. Elbeih, A.; Zeman, S.; Jungova, M.; Vávra, P. & Akstein, Z. Effect of different polymeric matrices on some properties of plastic bonded explosives. *Propellants, Explos. Pyrotech.*, 2012, **37**(6), 676-684. doi: 10.1002/prep.201200018
36. Tu, Z. & Lu, Y. Evaluation of typical concrete material models used in hydrocodes for high dynamic response simulations. *Int. J. Impact Eng.*, 2009, **36**(1),132-146. doi: 10.1016/j.ijimpeng.2007.12.010
37. Riedel, W; Thoma, K; Hiermaier, S. & Schmolinske, E. Penetration of reinforced concrete by BETA-B-500 Numerical analysis using a new macroscopic concrete model for hydrocodes. Ninth international symposium on the interaction of the effects of munitions with structures. 1999, 315.

CONTRIBUTORS

Dr Mohamed Abdelkhalik Aboelseoud obtained his PhD in Civil Engineering from Missouri University of Science and Technology. His current research focuses on: Hybrid composite beam bridges, behavior analysis of fiber-reinforced polymer (FRP) composites, the durability of FRP composites, blast mitigation, ballistic armors, electrically conductive cement-based materials, and structural analysis.
In the present study, he conducted Autodyn simulations, proposed several mitigation systems, and synthesized the current research results by crafting this manuscript.

Dr Tamer Elshenawy obtained his PhD from the University of Manchester, UK, in 2012. He has been working in the field of research in weapons, ammunition and explosives as well as rocket propulsion. Current researches include: Shaped charges design and developments as well as explosive manufacturing technologies.
In the current study, he contributed to proposing the mitigation structures. He also executed the experimental program.